AD-7/GBAR status report for the 2022 CERN SPSC

P. Blumer[1], M. Charlton[2], M. Chung[3], P. Cladé[4], P. Comini[5], P. Crivelli[1], O. Dalkarov[6], P. Debu[5], A. Douillet[4,7], P. Froelich[8], S. Guellati[4], P-A. Hervieux[9], L. Hilico[4,7], P. Indelicato[4], G. Janka[1], S. Jonsell[8], J-P. Karr[4,7], B. Kim[10], S. Kim[11], E-S. Kim[12], Y. Ko[10], T. Kosinski[13], N. Kuroda[14], B. Lee[11], H. Lee[11], J. Lee[10], E. Lim[12], L. Liszkay[5], D. Lunney[15], K. Lévêque[9], G. Manfredi[9], B. Mansoulié[5], M. Matusiak[13], M. Müller[1], V. Nesvizhevsky[16], F. Nez[4], S. Niang[5], B. Ohayon[1], K. Park[11], N. Paul[4], S. Procureur[5], P. Pérez[5], B. Radics[1], C. Regenfus[1], S. Reynaud[4], C. Roumegou[15], O. Rousselle[4], J-Y. Roussé[5], A. Rubbia[1], J. Rzadkiewicz[13], Y. Sacquin[5], F. Schmidt-Kaler[17], M. Staszczak[13], K. Szymczyk[13], T. Tanaka[14], B. Tuchming[5], B. Vallage[5], D.P. Van der Werf[2], A. Voronin[6], S. Wolf[17], D. Won[11], S. Wronka[13], Y. Yamazaki[18], K-H. Yoo[3]

(GBAR Collaboration)

[1] *Institute for Particle Physics and Astrophysics, ETH Zurich, 8093 Zurich, Switzerland*
[2] *Department of Physics, College of Science, Swansea University, Swansea SA2 8PP, United Kingdom*
[3] *Department of Physics, Ulsan National Institute of Science and Technology (UNIST), 50, UNIST-gil, Ulsan 44919, Republic of Korea*
[4] *Laboratoire Kastler Brossel, Sorbonne Université, CNRS, ENS-Université PSL, Collège de France, Campus Pierre et Marie Curie, 4, place Jussieu, F-75005 Paris, France*
[5] *IRFU, CEA, Université Paris-Saclay, F-91191 Gif-sur-Yvette, France*
[6] *P. N. Lebedev Physical Institute, 53 Leninsky Prospect, 119991 Moscow, Russia*
[7] *Université d'Evry-Val d'Essonne, Université Paris-Saclay, Boulevard François Mitterand, F-91000 Evry, France*
[8] *Department of Physics, Stockholm University, SE-10691 Stockholm, Sweden*
[9] *Université de Strasbourg, CNRS, Institut de Physique et Chimie des Matériaux de Strasbourg, UMR 7504, F-67000 Strasbourg, France*
[10] *Center for Underground Physics, Institute for Basic Science, 70 Yuseong-daero 1689-gil, Yuseong-gu, Daejeon 34047, Korea*
[11] *Department of Physics and Astronomy, Seoul National University, 1 Gwanak-Ro, Gwanak-gu, Seoul 08826, Korea*
[12] *Department of Accelerator Science, Korea University Sejong Campus, Sejong-ro 2511, 0019 Sejong, Republic of Korea*
[13] *National Centre for Nuclear Research (NCBJ), ul. Andrzeja Soltana 7, 05-400 Otwock, Swierk, Poland*
[14] *Institute of Physics, University of Tokyo, 3-8-1 Komaba, Meguro, Tokyo 153-8902, Japan*
[15] *Université Paris-Saclay, CNRS/IN2P3, IJCLab, Orsay, France*
[16] *Institut Max von Laue - Paul Langevin (ILL), 71 avenue des Martyrs, Grenoble, France, F-38042*
[17] *QUANTUM, Institut für Physik, Johannes Gutenberg Universität, D-55128 Mainz, Germany*
[18] *Ulmer Fundamental Symmetries Laboratory, RIKEN, 2-1 Hirosawa, Wako, 351-0198, Saitama, Japan*

CERN-SPSC-2022-003 / SPSC-SR-302
10/01/2022

Abstract

We report on the activities (including first data taking) performed during 2021 and the plans for 2022 for the GBAR experiment.

1 Introduction

The goals of GBAR for 2021 were to use protons to set up the apparatus, optimise processes, measure H and H^- production rates, test the Lamb shift measurement system, install the antiproton trap and then switch to antiprotons when available from ELENA to produce anti-hydrogen.

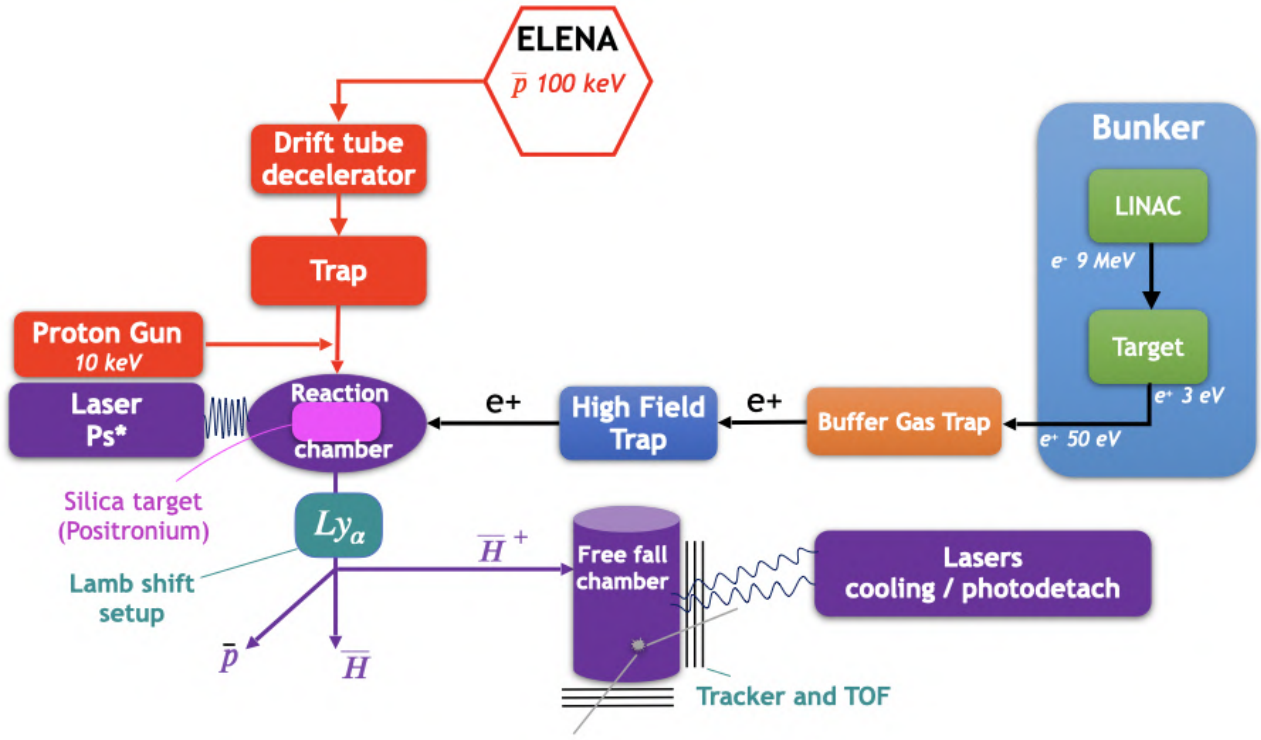

Figure 1: *Scheme of the GBAR experiment.*

We report below on the progress in installation of the apparatus in the AD hall at the LNE50 extraction beam line from ELENA. Figure 1 depicts the different parts of the experiment when fully installed. Namely the positron beam produced with a linac followed by two traps for e^+ accumulation, the antiproton beam delivered by ELENA being further decelerated with a pulsed-drift-tube, and the proton source allowing to study the matter reactions with positronium. Those beams are focused to the same point where positrons are converted into positronium, which can be excited using a laser pulse. Hydrogen or antihydrogen atoms are transported to a dedicated setup to measure their Lamb shift. The outgoing charged particles are separated employing an electrostatic switchyard. The chamber in which the free fall of anti-ions will take place is not yet made and is presently replaced by the antiproton trap, where it is tested before being transferred to its final position between the drift tube and the reaction chamber. Figure 2 shows the experimental zone.

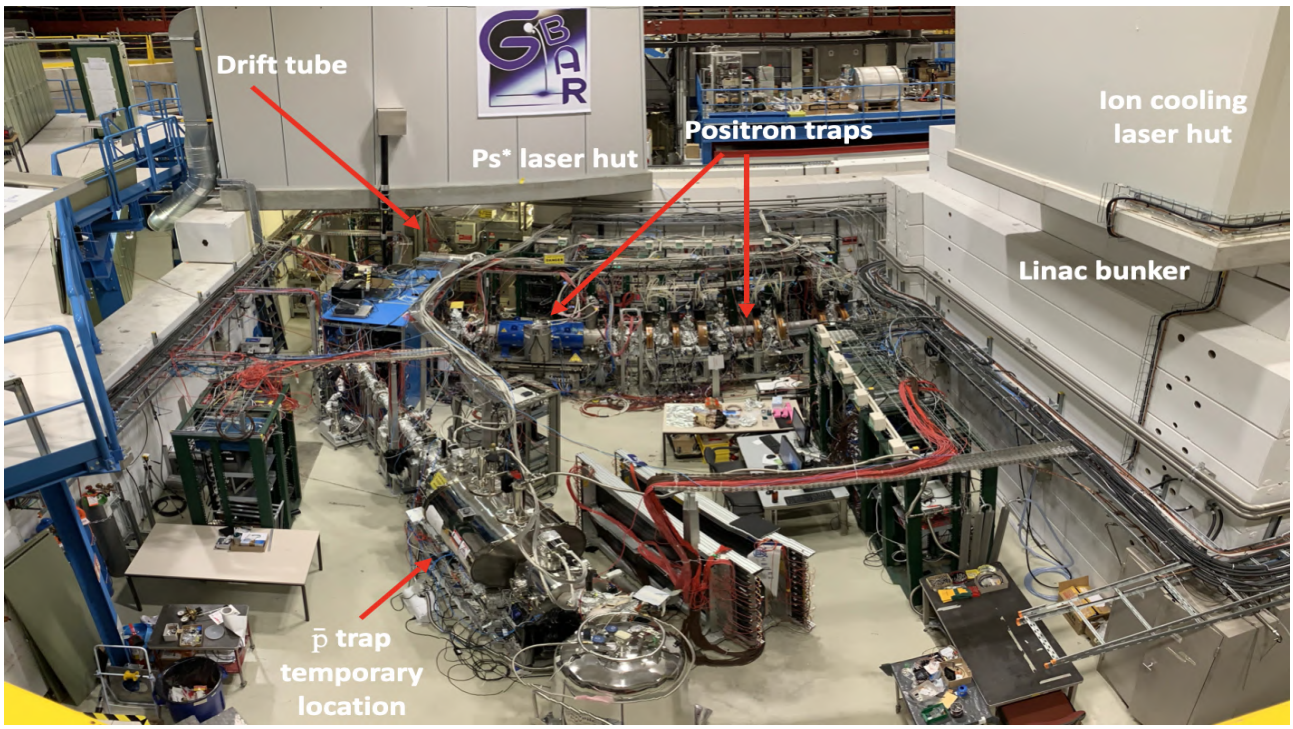

Figure 2: *Experimental zone.*

2 Positron Production

The positron beam is produced using a 9 MeV electron linear accelerator equipped with a water cooled tungsten target. The peak electron current is 300 mA, with a pulse length of 2.85 μs. The repetition rate can be varied from 1 to 300 Hz. In 2021, we mainly operated at 200 Hz because of a limitation in the gun modulator. The high energy positrons (MeV range) produced by pair creation in the target are moderated to typically 3 eV in a series of tungsten meshes located beneath the target and accelerated to 50 eV for further transport in a beam line. As described in a 2021 article published in NIMA [1], we typically ran with a flux of 4×10^7 slow positrons per second. The experts could not repair the gun modulator because of the pandemic during the first semester and later because there would be a risk that the linac would not be available, resulting in a loss of antiproton beam time. This work is scheduled to be performed in March 2022 together with other repairs due to radiation damage (dose up to 30 kGy/h). The accelerating structure will be exchanged with one with higher reliability and a better efficiency to transfer the RF power to the beam. This may also result in up to 20% increase in electron current.

3 Positron trapping

Positrons are trapped in a series of two traps. The Buffer Gas Trap (BGT) captures and cools the positrons using N_2 and CO_2 while the High Field Trap (HFT) is able to accumulate them for long durations at a much lower pressure. In 2020 a total of 10^9 e^+ were accumulated in 1100 s [2]. In 2021 routine operation was obtained with 1.5×10^8 e^+ per 110 s to match the antiproton cycle. A pumping restriction was installed to better protect the linac against the BGT gases. A test was performed replacing the N_2 gas in the BGT by a solid SiC remoderator. We had demonstrated that this material provides a moderation efficiency in the 60-70% range below 1 keV incident energy of the positrons [3] and confirmed this result for the energy range used at CERN (Figure 3). The test showed that the trapping efficiency was increased by a

factor 3 reaching 40% (Figure 3). The test consisted in placing a plate of SiC between stage 2 and stage 3 of the BGT, thus preventing further transport to stage 3 and the HFT. A system is under study to implement a moveable plate to allow transferring the positrons downstream or to use the diocotron mode of the positron cloud to move it radially away from the plate.

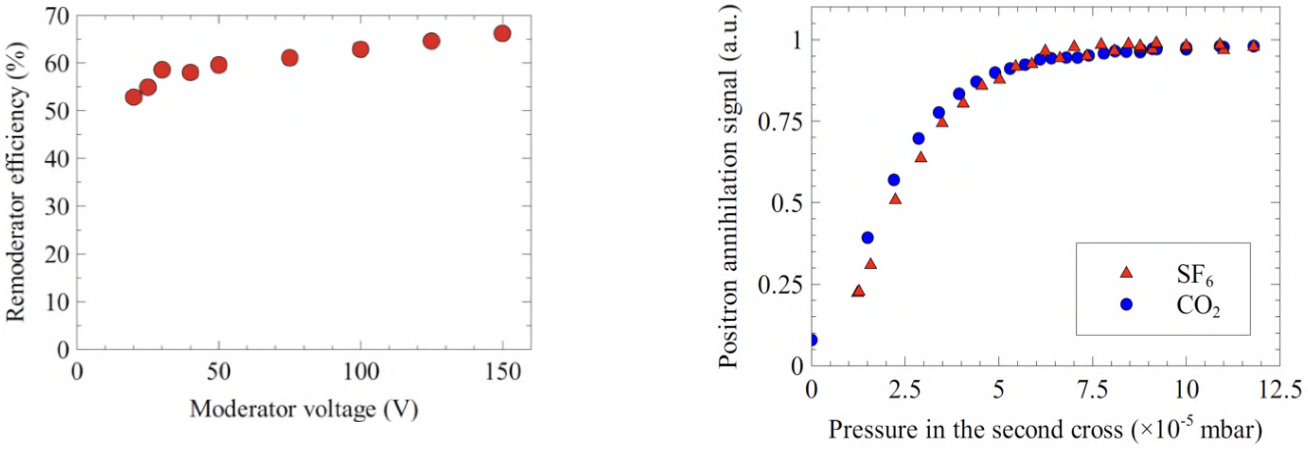

Figure 3: *Moderation efficiency of the SiC sample as a function of incoming positron energy (left). Trapping efficiency in the BGT with SiC replacing N_2 as a function of pressure with CO_2 or SF_6 as cooling gases. The normalisation of the vertical axis corresponds to 40% maximum trapping efficiency (right).*

4 Positronium production

In order to create a dense positronium cloud, the accumulated positrons must be ejected from the HFT and focused onto a small target where they are converted into ortho-positronium. A sample holder (Figure 4), located at the centre of the reaction chamber (RC), holds several targets to form positronium. Ps is produced by interaction of the positron bunch with a specially treated silica film. One target is formed of a simple flat silicium surface. Another has also a flat surface with a specially treated film to form oPs. There is also a square tube ($2 \times 2 \times 20\,\mathrm{mm}^3$) to contain Ps with one plane made with the same silica film, one plane with a thin Si_3N_4 window and two planes made of standard silica (Figure 5). A mirror directs a laser beam for the later study with Ps excitation. An MCP intersects the positron beam to check its focussing.

The magnetic field intensity at the centre of the HFT is 5 T. Its fringe field affects the antiproton beam transport to the positronium target. A magnetic shielding box made of soft iron surrounds the target location, reducing the field intensity at the target from 2 mT to about 0.4 mT. The positron bunch is ejected from the trap at 300 eV energy and further accelerated with a pulsed drift tube to 4 keV to optimise conversion into positronium (Figure 6). The bunch length is 25 ns. After traversing the magnetic shield wall, the beam is focused using a set of cylindrical electrodes and two planar electrodes to shape the beam flat to adapt to the Si_3N_4 window. This passage through the wall is not adiabatic and is very delicate. We estimate that about 70% of the positron intensity is lost in part at the location of this passage and near the flat electrodes. This is due in part to the beam diameter in the HFT, which is presently 0.8 mm FWHM and to the adjustment of iron plates at the passage of the magnetic shield that needs to be further optimised. The plasma size in the HFT is probably due to imperfect alignment of the magnetic axis with the axis of the electrodes. About 5×10^7 positrons from each ejection

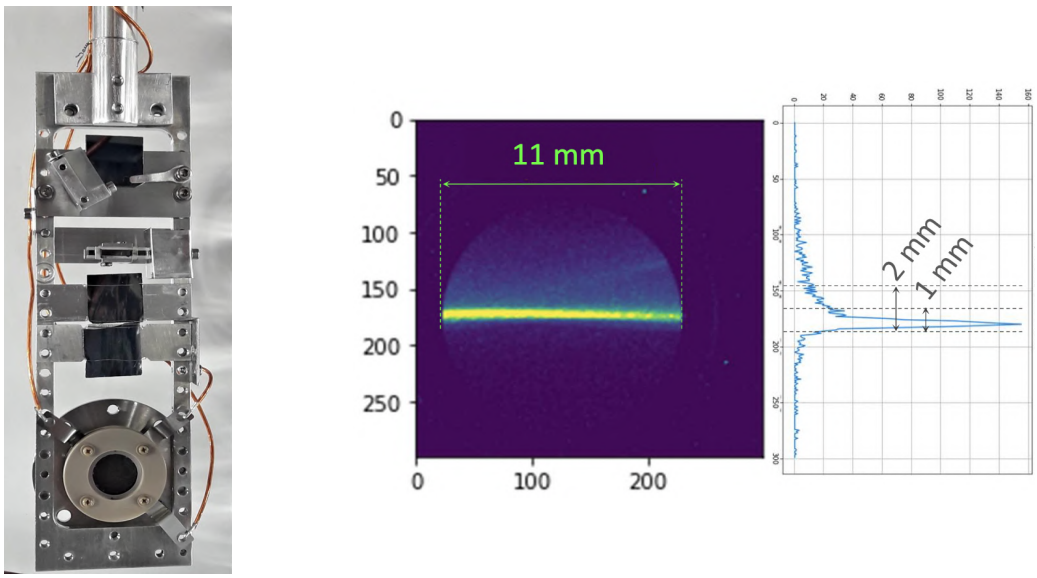

Figure 4: *Sample holder with different targets and an MCP to image the positron beam (left). Positron beam profile seen by this MCP (right).*

from the HFT reach the MCP. The number of oPs formed inside the cavity is presently not well measured, with estimates reaching a maximum of 5×10^6. Work is underway to correct for the defects and effectively use the presently available positron flux, including the increase of efficiency due to the SiC based e^+ capture, to reach of the order of 10^8 oPs.

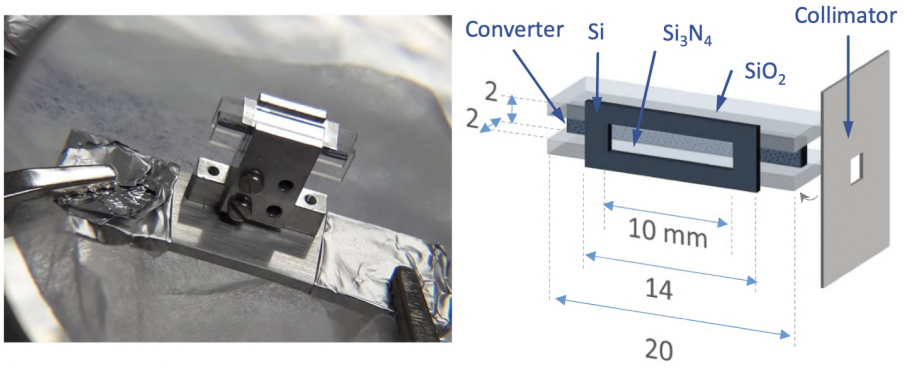

Figure 5: *Cavity target for Ps production.*

5 Antiproton deceleration and trapping

In 2021, the antiproton trap was placed at the end of the beam line for commissioning studies, including proton and antiproton trapping without disturbing the other parts of the experiment. Electron trapping was demonstrated, but it was not yet possible to test hadron trapping due to technical problems in the beam transport (see also end of this section). The trap was replaced at its nominal location by a so-called connection line equipped with electrostatic lenses and steerers as well as MCPs to image the beam (Figure 7).

We use a drift tube to decelerate the antiprotons to energies below 10 keV, suitable for trapping and producing antihydrogen. This device was the subject of another 2021 publication in NIMA [4]. This tube is held at more than 90 kV for 0.5 s before the antiproton bunch arrives, and is then switched to ground in less than 30 ns while the particles are traversing it [4]. In

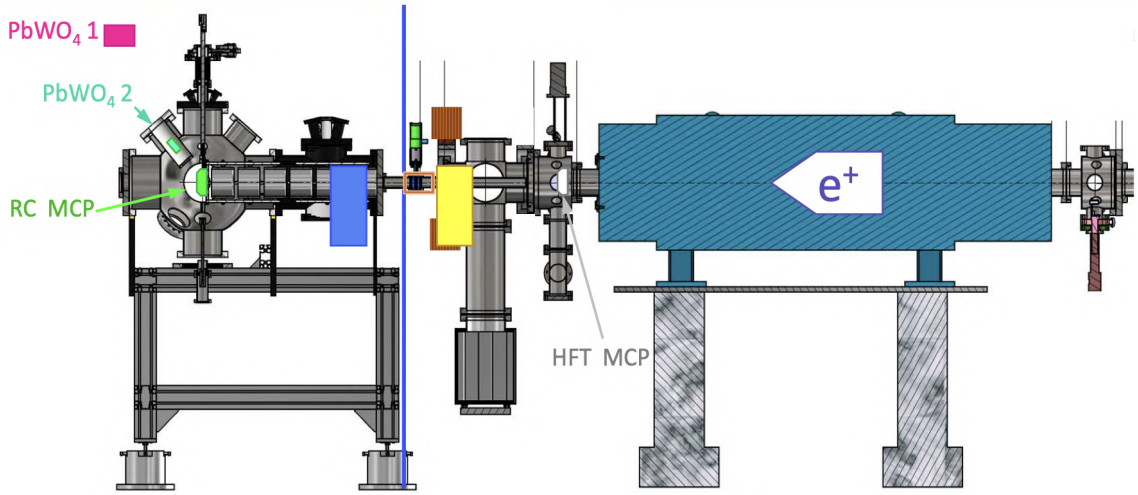

Figure 6: *Side view of the transport of positrons to the positronium target. The HFT at the right ejects its stored positrons at an energy of 300 eV. The drift tube is located in the central cross. The vertical blue line represents the iron wall of the magnetic shielding box in which a set of 6 cylindrical electrodes focus the beam to the target position at the centre of the spherical reaction chamber where they are converted into positronium. Several detectors are located around the target. An MCP (green) images the positron beam spot when the target is away from the beam axis. Two* $PbWO_4$ *crystals (pink and green) are also placed close to the interaction point. Two plastic scintillator plates are located upstream(yellow) and downstream (blue) the shielding wall.*

contrast with experiments using a degrader foil, we are thus very sensitive to the beam quality. We interacted very fruitfully with the AD/ELENA team to optimise procedures and obtain a beam usable for physics. A 100 keV beam of H^- ions had been delivered from ELENA to GBAR in 2020 to commission the LNE50 beam line, and allowed to test the drift tube and succesfully decelerate the ions to 8 keV. In 2021, we benefited again from the availability of H^- ions with a repetition rate every 15 s, extensively used to tune the numerous voltages of the steering and focussing electrodes along our 11 m long beam line, while this would have been extremely time consuming with only the antiprotons since their repetition rate was about every 110 s. The momentum spread was 0.5×10^{-3}, the bunch length was 65 ns (standard deviation), the horizontal and vertical emittances ranged between 2 and 2.5 μm (RMS), and the extraction time jitter was 5 ns. At the end of the beam time, bunch rotation was applied reducing the bunch length to 40 ns. This ensures that the entire bunch length is well contained within our 45 cm drift tube while it is switched to ground.

For the 2021 run, we replaced several parts of the drift tube setup, in particular the supports and junctions between the insulating and metallic parts, so that the sparking rate was reduced drastically. Figure 8 shows an example of $\overline{p}$ deceleration detected at 11 keV with the pulse seen on MCP2 (indicated in Fig. 7) located after the drift tube together with the trigger for the 100 kV switch.

We observed a current drawn on the voltage supply of the drift tube, probably due to field emission. This results in a drop of the voltage applied to the drift tube, and was corrected for in the estimate of the energy of the decelerated particles. Near the end of the antiproton beam period, this current increased suddenly, inducing a voltage drop such that we could not decelerate below 20 keV. The steering electrodes downstream the drift tube had been chosen to match an energy below 10 keV. We thus had to run far from optimal reaction cross section energy with non optimal focusing during the last weeks of the run, i.e. approximately only 10%

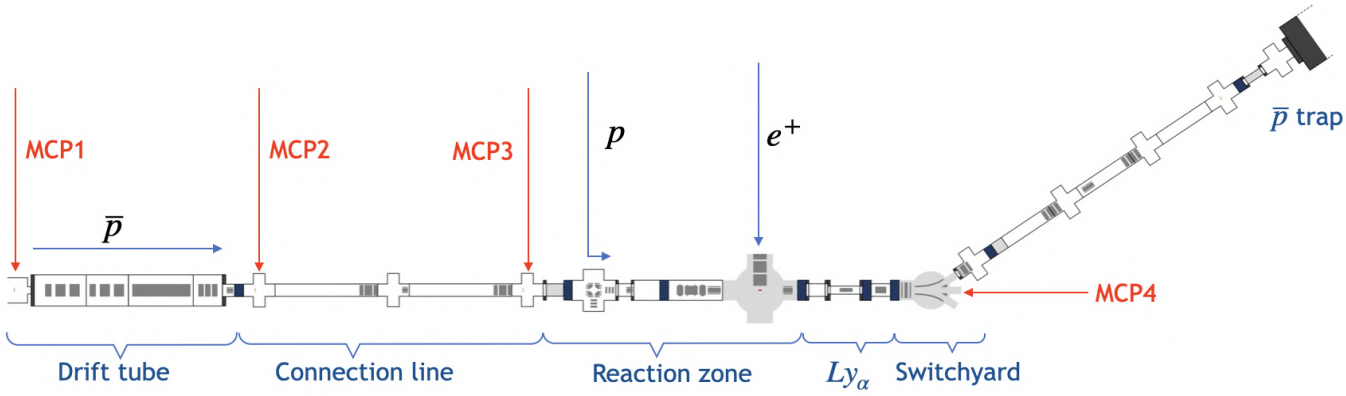

Figure 7: *GBAR $\bar{p}$ beam line in 2021. Upstream at left, the drift tube is surrounded by two MCP's as beam diagnostics. An ECR source provides a proton beam directed towards the spherical reaction chamber where e^+ are converted into oPs. The Lamb shift setup located downstream this chamber is followed by an electrostatic switchyard. The trap is located at the end of the line and replaced by an electrostatic connection beam line.*

of the antiproton intensity was focused onto the cavity hosting the positronium target. It was not possible to steer the beam efficiently down to the antiproton trap.

6 Commissioning of the Lamb shift setup

A 2.45 GHz ECR source delivers an ion beam from a small H_2 cartridge. It was operated to produce a beam of 8 keV energy and a current of 5 μA of protons with a 100 ns pulse length, i.e 3×10^6 protons per bunch. The beam was focused onto a 12 nm thick carbon foil where about 80% of the protons are converted into neutral H [5]. Around 10% of these H are in the meta-stable 2S state, which has a lifetime of 0.12 s and therefore are useful for the Lamb shift measurement. H(2S) can be in different F = 0,1 states as shown in Figure 9.

The apparatus has been commissioned at PSI to measure the Lamb shift of muonium [6]. It comprises two microwave transmission lines, electric field for quenching and four MCP detectors specially coated to detect Ly_α photons (Figure 9). Microwaves were generated to induce the $2S \rightarrow 2P$ transition with frequencies ranging from 700 to 1600 MHz. The 2P state decays with a lifetime of 1.6 ns. The 2S states surviving the microwave field are quenched by an electric field produced by ring electrodes. The Ly_α photon is detected in one of the four MCPs located around the beam axis. To extract the line shape of the Lamb shift the ratios of microwave-on vs. microwave-off signals were calculated separately for each MCP. To obtain the fitting curve the two hyperfine distances of 177 MHz (2S) and 59 MHz (2P) were fixed. The result for the resonance is 1080.1 ± 13.5 MHz, the theoretical value is around 1088 MHz. With this value the hydrogen Lamb shift can be calculated with $(1080.1 - 0.25 \times 177 + 0.25 \times 59)$ MHz which results to 1050.5 ± 13.5 MHz. Theoretically the value lies at 1057.8341 ± 0.0002 MHz [7]. A measurement was performed in a test run in the GBAR beamline using the proton source described above with the carbon foil to produce the hydrogen atoms. The result displayed in Figure 10 is compatible with the known value.

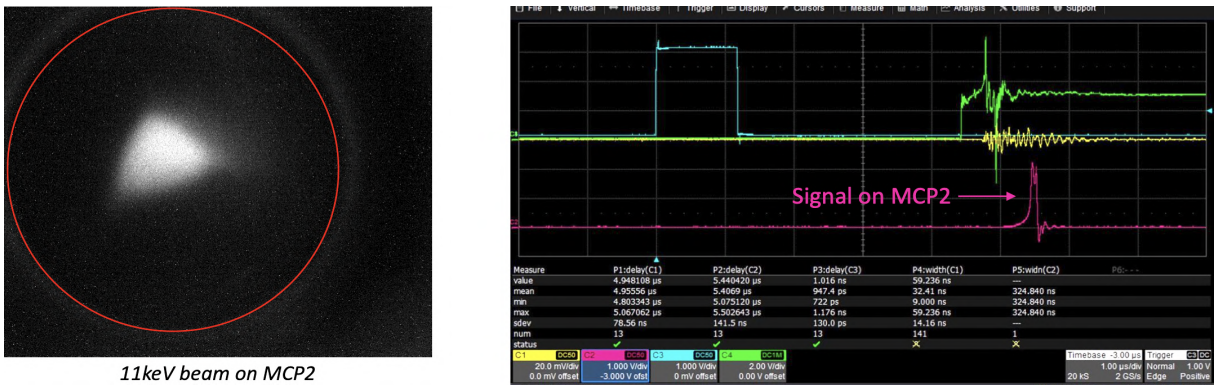

Figure 8: *Beam spot (left) and waveform (right) of the decelerated $\overline{p}$ beam. The green pulse is from the HV switch (1 μs per division)*

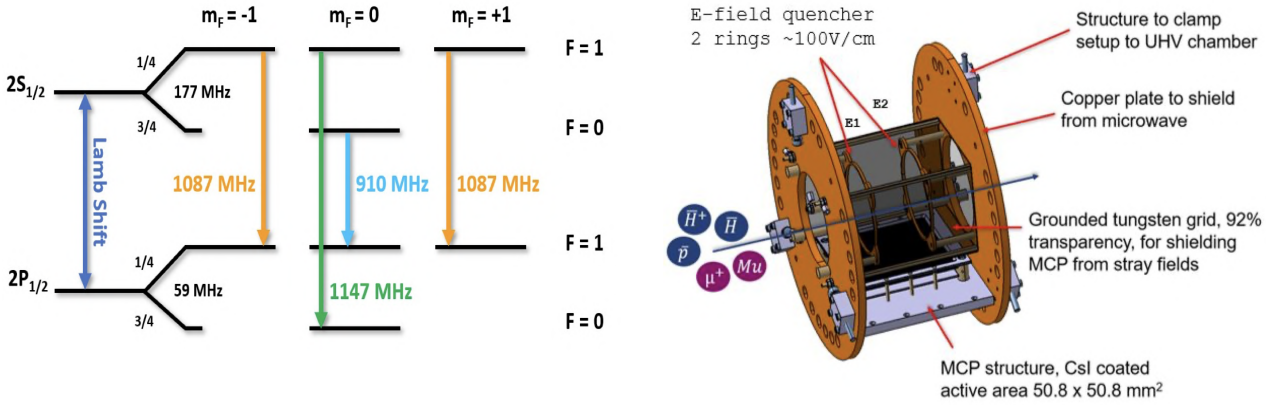

Figure 9: *Theoretical Lamb Shift transitions (left). MCP detector (right).*

7 Combining $\overline{p}$ and e^+ beams in running conditions

The formation of antihydrogen by interaction of antiprotons with positronium is maximum at an incident energy of 6 keV [8] [12]. The concerted operation of the main components of the experiment to mix $\overline{p}$ and Ps was achieved. As mentioned in the previous sections, due to the problems with the drift tube in the last days of the run the antiproton beam energy was set at 20 keV with poor focusing and energy dispersion, thus, only about 10% of the antiproton bunch could be guided onto the reaction tube. Further, the positrons could not be fully transmitted to the target due to the stray magnetic field from the HFT, producing of the order of 5×10^6 Ps per spill. Using the formation cross-section at these energies (smaller at 20 keV than at 6 keV, by a factor of 5) [8] [9], we estimate that about 1 antihydrogen atom was formed every 100 crossings. Hence above all, this was a first measurement of the backgrounds, which consist mainly of signals from delayed (several μs) pbar annihilation products or late gammas from the oPs annihilation tail.

An electric field right after the $\overline{\mathrm{H}}$ formation region was used to deflect charged particles from the straight trajectory of neutral particles. Antihydrogen candidate events were detected with MCP4 located after the on-axis exit of the switchyard (see Figure 7) in a 1 μs time window, corresponding to the arrival time of neutral particles of beam energy and originating at the interaction point. This MCP provided both an image and an electric signal (Figure 11). Pedestals were taken during the first 2 μs of each spill and events selected with a signal greater than 3 standard deviations above the pedestal. We recorded data alternatively with only

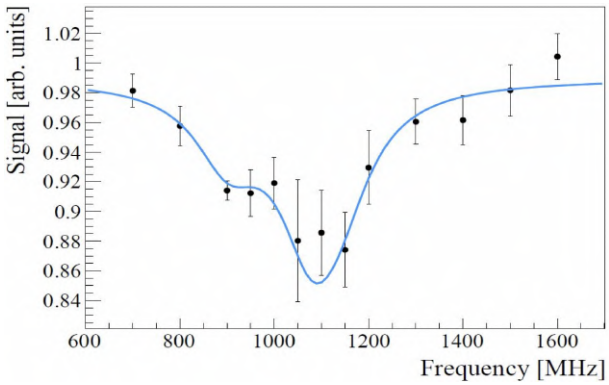

Figure 10: *Lamb shift hydrogen data with fit.*

antiprotons, with only positronium, and with both mixed. We also took data without those beams, but with the AD/ELENA rings running in order to check for backgrounds emanating from the antiprotons circulating there.

The background runs totalled 14 events selected out of 137 $\overline{p}$ only spills, 6 events out of 196 e^+ only spills, and zero events out of 57 spills with AD/ELENA only. During the 247 mixing spills, 32 events were selected, which is comparable to the background measurement.

With a well-focused 6 keV antiproton beam, fully transmitted positrons, and using the SiC remoderator, yielding 10^8 Ps per spill, we expect the formation of about 4 antihydrogen atoms per spill that we can measure with our validated setup in 2022.

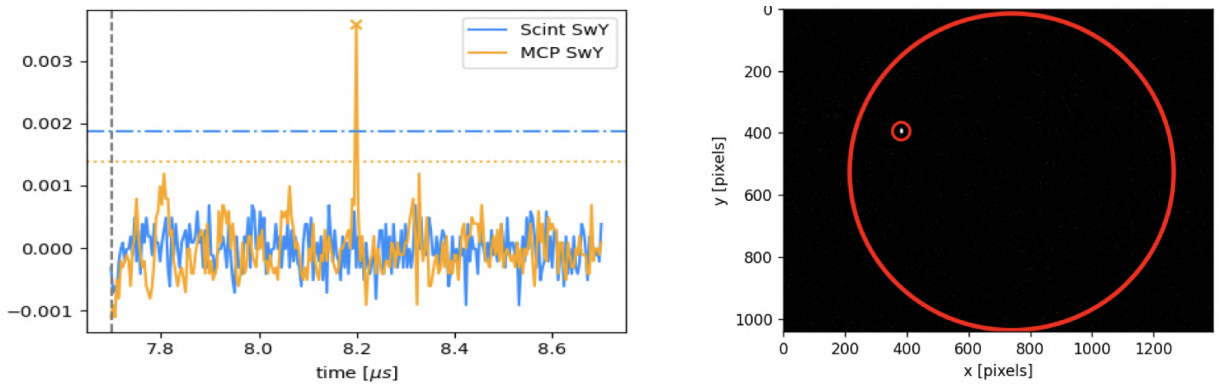

Figure 11: *Example of event detected by the MCP for antihydrogen events. Electric signal (left). Image with single hit (right).*

8 Outlook

The H^- beam from ELENA was extensively used to adjust the parameters of the beam optics from the ELENA extraction LNE50 line to within our experimental zone. This tool remains very important for the coming years since its repetition rate is 7 times greater than that with antiprotons. We achieved deceleration of the ELENA beam below 10 keV and routine operation of our positron beam. While the antiproton trap commissioning is still in progress, we have had first trials at mixing particles and measured the backgrounds to antihydrogen detection from the antiprotons, the positrons and positronium as well as from cosmic rays and the AD/ELENA facility. Work is necessary to solve the problem of field emission that reduces the performance of the deceleration drift tube. The device is being inspected on a dedicated vacuum chamber

and parts tested individually at high voltage to identify the source of electron emission. As well, the transport of the positrons and their accumulation must be improved.

Our proton source will enable studying the reactions with protons replacing the antiprotons and start commissioning the antiproton trap, before the run resumes in May. The trap will then be commissioned with antiprotons in its present location, and moved, when ready, to its final position. The main goals for 2022 remain to produce antihydrogen atoms via the charge exchange reaction of antiprotons on positronium and to detect the Lamb shift transition.

9 Activities in the collaborating institutes

In the home laboratories, work has been minimal due to the pandemic, and concentrated on design, simulations and theoretical work [10, 11, 12, 13, 14].

Acknowledgements

We thank F. Butin and the EN team, L. Ponce and the AD/ELENA team for their fruitful collaboration.

References

[1] M. Charlton et al., Nuclear Inst. and Methods in Physics Research, **A 985** (2021) 164657

[2] S. Niang, PhD thesis, Paris-Saclay University, France (2020); S. Niang et al., Acta Physica Polonica A 137, 164-166 (2020)

[3] A.M.M Leite, P. Debu, P. Pérez, J-M. Reymond, Y. Sacquin, B. Vallage and L. Liszkay, Journal of Physics: Conf. Series **791**, 012005 (2017)

[4] A. Husson et al., Nuclear Inst. and Methods in Physics Research, **A 1002** (2021) 165245

[5] M. Gonin, R. Kallenbach and P. Bochsler, Review of Scientific Instruments **65**, 648 (1994)

[6] B. Ohayon et al., Phys. Rev. Lett. **128**, 011802 (2022)

[7] V. A. Yerokhin, K. Pachucki, V. Patkós, Ann. Phys. **2019**, 531

[8] C.M. Rawlins, A.S Kadyrov, A.T. Stelbovics, I. Bray and M. Charlton, Physical Review **A 93**, 012709 (2016)

[9] K. Lévêque-Simon, PhD Thesis, University of Strasbourg, France (2020); P. Comini, PhD Thesis, Université Paris VI, Pierre et Marie Curie, France (2014)

[10] T. Yamashita, Y. Kino, E. Hiyama, S. Jonsell and P. Froelich, *Near-threshold production of antihydrogen positive ion in positronium–antihydrogen collision*, New Journal of Physics **23**, 012001 (2021)

[11] K. Lévêque-Simon and P-A Hervieux, *Charge exchange three- and four-body reactions in the presence of a laser field*, J. Phys.: Conf. Ser. **1412** 222007 (2020)

[12] P. Comini, P-A. Hervieux and K. Lévêque-Simon, Corrigendum: $\overline{H}^+$ *ion production from collisions between antiprotons and excited positronium: cross sections calculations in the framework of the GBAR experiment*, New J. Phys. **23** 029501 (2021)

[13] O. Rousselle, P. Cladé, S. Guellati-Khélifa, R. Guérout, S. Reynaud, *Analysis of the timing of freely falling antihydrogen*, arXiv:2111.02815

[14] O. Rousselle, P. Cladé, S. Guellati-Khélifa, R. Guérout, S. Reynaud, *Improving the statistical analysis of anti-hydrogen free fall by using near edge events*, arXiv:2111.06722